IEEE Access
Multidisciplinary | Rapid Review | Open Access Journal

Received June 10, 2021, accepted June 16, 2021, date of publication June 23, 2021, date of current version July 5, 2021.

Digital Object Identifier 10.1109/ACCESS.2021.3091872

Dual-Comb Spectrometer Based on Gain-Switched Semiconductor Lasers and a Low-Cost Software-Defined Radio

CLARA QUEVEDO-GALÁN, ANTONIO PÉREZ-SERRANO, IGNACIO E. LÓPEZ-DELGADO, JOSE MANUEL G. TIJERO, AND IGNACIO ESQUIVIAS

CEMDATIC-E.T.S.I. Telecomunicación, Universidad Politécnica de Madrid (UPM), 28040 Madrid, Spain

Corresponding author: Clara Quevedo-Galán (clara.quevedo.galan@upm.es)

This work was supported in part by the Ministerio de Economía y Competitividad of Spain, LIDERA, under Grant RTI2018-094118-B-C21, in part by the Universidad Politécnica de Madrid/Comunidad de Madrid, MULTI-GAS-PIC, under Grant APOYO-JOVENES-KXHJ8C-16-VCKM78, and in part by the Comunidad de Madrid and FEDER Program under Grant SINFOTON2-CM (P2018/NMT-4326).

ABSTRACT Dual-comb spectroscopy has become a topic of growing interest in recent years due to the advantages it offers in terms of frequency resolution, accuracy, acquisition speed, and signal-to-noise ratio, with respect to other existing spectroscopic techniques. In addition, its characteristic of mapping the optical frequencies into radio-frequency ranges opens up the possibility of using non-demanding digitizers. In this paper, we show that a low-cost software defined radio platform can be used as a receiver to obtain such signals accurately using a dual-comb spectrometer based on gain-switched semiconductor lasers. We compare its performance with that of a real-time digital oscilloscope, finding similar results for both digitizers. We measure an absorption line of a $H^{13}C^{14}N$ cell and obtain that for an integration time of 1 s, the deviation obtained between the experimental data and the Voigt profile fitted to these data is around 0.97% using the low-cost digitizer while it is around 0.84% when using the high-end digitizer. The use of both technologies, semiconductor lasers and low-cost software defined radio platforms, can pave the way towards the development of cost-efficient dual-comb spectrometers.

INDEX TERMS Dual-comb spectroscopy, optical frequency comb, semiconductor lasers, software defined radio.

I. INTRODUCTION

Optical Frequency Combs (OFCs) have attracted a lot of attention during the last decades due to their vast number of applications in many different fields [1]. An OFC is a coherent optical spectrum generated by a laser source, consisting of equally spaced narrow spectral lines with a given repetition rate (f_R). OFCs have been found especially suitable for applications such as molecular spectroscopy [2], telecommunications [3], radio-frequency (RF) generation [4], and distance measurement [5]–[7] among others.

In the field of molecular spectroscopy, dual-comb spectroscopy (DCS) has become one of the most appealing techniques since it offers advantages over conventional spectrometers such as the absence of moving parts, the improvement of frequency resolution, accuracy, acquisition speed, and signal-to-noise ratio (SNR), as well as a great potential to be implemented in compact systems [8]. The basic concept of DCS, which is depicted in Fig. 1, consists in using two OFCs with slightly different repetition frequencies (f_R and $f_R + \Delta f_R$) that interact with an absorbent medium before interfering in a photodiode, where they generate an electrical RF comb [9]. Therefore, the result is a RF comb that maps the absorption that takes place in the optical frequency range into a down-converted electrical frequency range, thus making the measurements simpler.

In order to obtain cost-effective dual-comb spectrometers, semiconductor lasers are a suitable choice of light source due to their well-known intrinsic benefits in terms of compactness, integrability, electrical pumping, high efficiency, and low cost. Gain-switching (GS) of semiconductor lasers is a technique to generate high-quality OFCs featuring a great flexibility in the selection of the repetition rate as well as easy implementation, robustness, and stability [10].

The associate editor coordinating the review of this manuscript and approving it for publication was Norbert Herencsar.

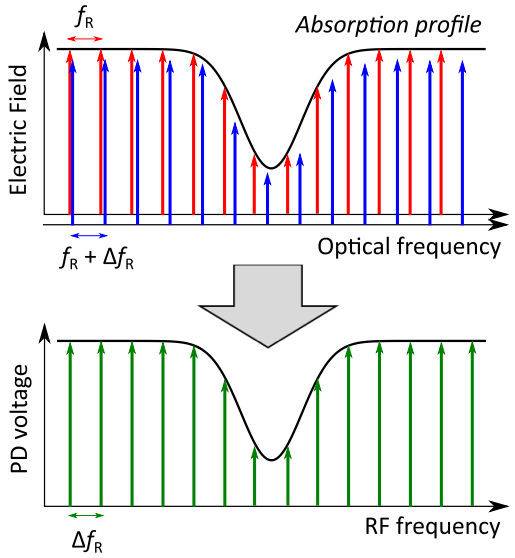

FIGURE 1. Dual-comb spectroscopy concept. Two optical frequency combs with slightly different repetition rates, f_R and $f_R + \Delta f_R$, interact with an absorption profile at optical frequencies. Its beating is detected with a photodiode (PD), mapping the absorption profile that takes place at optical frequencies into the radio-frequency (RF) domain. Adapted from [9].

This technique consists in modulating a laser with a superposition of two electrical signals: a DC bias current and a large amplitude AC current at a repetition rate f_R. Usually, a sinusoidal AC current is employed for repetition rates of the order of the laser relaxation oscillations, $f_R \sim 5 - 25$ GHz [11], [12]. To obtain OFCs at lower repetition rates, $f_R \sim 100 - 500$ MHz, GS is usually accompanied by optical injection (OI) from an external laser in a master-slave configuration, in order to lock the phases of both lasers and preserve the coherence of the generated pulse train [13], [14]. We have recently demonstrated that the use of pulsed electrical excitation, instead of sinusoidal AC current, improves the width and flatness of low-frequency OFCs [15]. Combining OI with the use of a pulse pattern generator (PPG) as switching source, we obtained OFCs with 866 tones within 10 dB at $f_R = 100$ MHz [15]. These combs have proven to be useful to perform high-resolution molecular spectroscopy using the DCS technique [16].

In the quest for cost-efficient field deployable DCS systems, the use of semiconductor lasers as well as the photonic integration of these devices [17] seems a rather natural choice. In addition, these systems should be based on low-cost electronics for generating the different required signals without compromising the robustness, resolution, and accuracy of the system. In this direction, the viability of using step-recovery diodes for producing OFCs has been recently demonstrated [18]. To complete the entire picture, on the detection side, the analysis of the received RF spectrum should be also optimized in terms of cost. It is in this respect where the possibility of using software-defined radio (SDR) platforms comes into the scene. In a SDR platform some blocks of analog steps performing RF signal processing are replaced by software, thus avoiding undesirable effects such as thermal noise or voltage drifts. The maturity and versatility of SDR systems has progressively increased at concurrently lower cost up to make them appealing tools for the acquisition and processing of RF signals at low cost. These flexible signal processing platforms have already proven to be very useful in the field of nuclear magnetic resonance (NMR) spectroscopy [19], [20], frequency modulation spectroscopy [21], heterodyne interferometry [22], and stabilization of OFCs [23].

In this paper, we report a dual-comb spectrometer with externally injected gain-switched semiconductor lasers as OFC generators and a low-cost (sub $ 20) SDR platform in the receiver end of the system. We demonstrate, for the first time to the best of our knowledge, that DCS systems can be based on SDR platforms by experimentally measuring the absorption spectrum of a $H^{13}C^{14}N$ gas cell. Moreover, we compare the performance of the SDR platform with a high-quality oscilloscope as a digitization system. In this way, we prove that SDR platforms, besides reducing the cost of the system, are quite appropriate in terms of range of RF carrier and bandwidth to digitize the RF combs used in dual-comb applications.

II. EXPERIMENTAL SETUP

The experimental setup is shown in Fig. 2, and a photograph of the optical and optoelectronic components is shown in Fig. 3. The OFCs are generated by GS two single longitudinal mode semiconductor lasers: a discrete mode laser (DML, Eblana Photonics EP1550-0-DM-H19-FM) and a distributed feedback (DFB) laser (Gooch & Housego AA0702-193414-010-SM900-FCA-50). The two of them act as slave lasers, denoted as SL1 and SL2, respectively. Each slave laser is driven with the superposition of a DC bias current I^{DC} and an AC pulse train generated by a PPG (Anritsu MU181020A) with peak-to-peak voltage amplitude V^{AC}, repetition rate f_R, repetition rate difference Δf_R, and pulse width t_{pulse}. A narrow linewidth tunable laser (Pure Photonics PPCL300) acts as the master laser, whose optical signal, after being attenuated, is injected into the slave lasers using optical circulators. Polarization controllers are used to maximize the coupling in the master-slave configuration and subsequently, the beating between the two OFCs. An acousto-optic modulator (AA Opto-Electronic MT80-IIR30-Fio-PM0) is used to shift the frequency of the OFC generated by SL2 a value $f_{shift} = 80$ MHz. The reason for this frequency shift is threefold. Firstly, it minimizes the effects of the $1/f$ noise by shifting the heterodyne signal away from DC [24]. Secondly, it ensures that the beat notes produced at both sides of the spectrum around the injection can be unambiguously distinguished. And thirdly, it allows the use of a SDR platform by frequency shifting the signal into its tuning range.

After the acousto-optic modulator, both OFCs are coupled together in the same fiber and routed by two optical switches either to a reference path or through the gas cell. This system architecture is the so-called symmetric (collinear) configuration and it provides only the sample absorption [9]. The gas

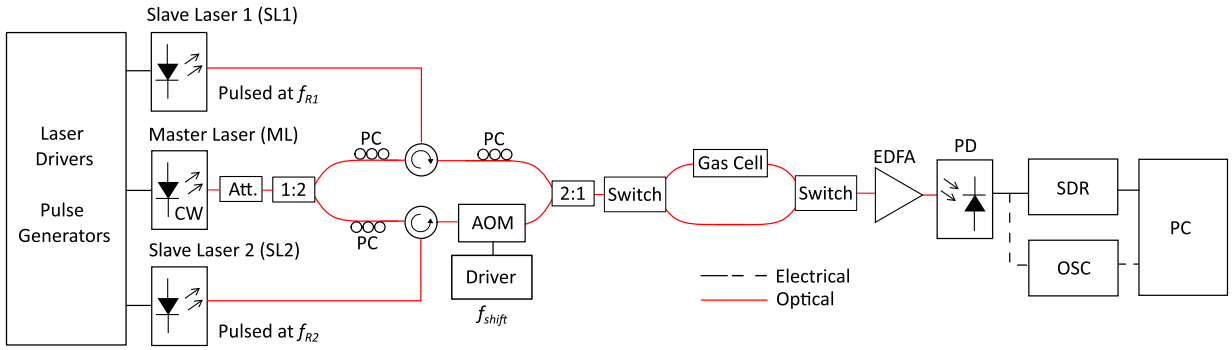

FIGURE 2. Experimental setup of the dual-comb spectrometer based on a master laser (ML) and two slave lasers (SL1 and SL2) which are gain-switched at f_{R1} and f_{R2} repetition rates, respectively. The spectrometer is implemented in a symmetric configuration, i.e. both combs pass through the gas cell or though the reference path depending on the optical switches. The RF comb detected at the photodiode (PD) is measured either with a software-defined radio (SDR) platform or with a real-time digital oscilloscope. Att.: Attenuator; PC: Polarization controller; AOM: Acousto-optic modulator; EDFA: Erbium doped fiber amplifier.

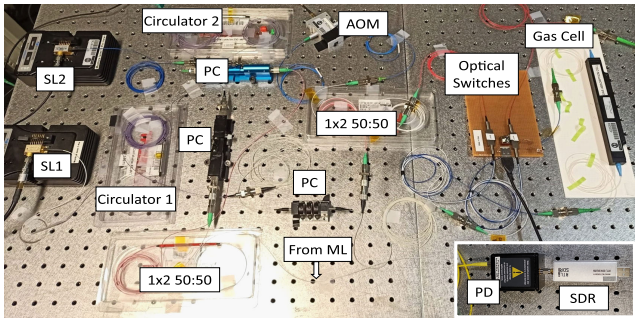

FIGURE 3. Photograph of the experimental setup in which the optical components are shown. An inset showing the receiver end of the system, photodetector (PD) and software-defined radio (SDR), is included.

cell (Wavelength Reference HCN-13-H(16.5)-25-FCAPC) contains $H^{13}C^{14}N$ at a pressure of 25 Torr and has an absorption length of 16.5 cm. The P(10) line at $\sim$ 1,549.73 nm is selected for the measurements. After passing through the gas cell, the optical signal is amplified by an Erbium doped fiber amplifier (EDFA, Amonics AEDFA-13-B-FA) and converted to the electrical domain using a 45 GHz photodiode (New Focus 1014). Both path lengths are much shorter than the coherence length of the master laser and therefore the coherent beating is preserved.

The resulting electrical signal, the RF comb, is measured either with a real time 20 Gsamples/s 10-bit digital oscilloscope (Keysight MSOS804A) or with a 3.2 Msamples/s 8-bit SDR platform. In the case of the measurements performed with the oscilloscope, the acquisition is triggered using a trigger obtained by mixing the signals from the two PPGs with a RF mixer to get the frequency difference. In addition, a common 10 MHz reference is used for the two PPGs and for the oscilloscope. The SDR receiver platform used (RTL-SDR BLOG V3) [25] is one of the most affordable on the market. It is based on the Rafael Micro R820T Silicon Tuner [26] and the Realtek RTL2832U DVB-T coded orthogonal frequency division multiplex (COFDM) demodulator [27]. Both chips were originally developed for consumer grade digital TV receivers, but the amateur radio operators community found out that these devices could be operated in a 'test mode' by bypassing the DVB-T decoding stage. This enables the device to be used as a generic programmable SDR. In these conditions, its tuning range spans from 25 MHz to 1.75 GHz, its bandwidth is 3.2 MHz and it produces raw 8-bit in-phase and quadrature (IQ) data samples [28]. The RF comb centered in f_{shift}, is received through the antenna port of the SDR. The R820T down converts the RF signal at a chosen center frequency to an intermediate frequency (IF) ($f_{\text{IF}} = 3.57$ MHz) with a voltage controlled oscillator (VCO). The RTL2832U controls the VCO so that the resultant signal at f_{IF} contains the RF comb. In the RTL2832U, the IF signal is filtered and sampled at 28.8 Msamples/s. The digital signal is demodulated with a quadrature demodulator, centered at f_{IF}, in order to obtain baseband IQ samples of the RF comb. Along this process several filtering and amplification stages are applied. Then, the samples are decimated to reduce the sampling rate to a configurable value, smaller than 3.2 Msamples/s. The decimation also reduces the bandwidth of the signal. The communication between the SDR platform and the computer is performed using MATLAB and Simulink. A Simulink hardware support package [28] including an interface with the RTL-SDR receiver is used. This interface enables the configuration of parameters such as the RF center frequency, the sampling rate, the number of samples or the tuner gain. In contrast with the acquisition performed with the real-time oscilloscope, the SDR platform has no trigger input, so it is not synchronized with the PPG signals. Finally, the samples resulting from any of the two acquisition methods are post-processed by a computer running MATLAB.

III. RESULTS

The operation conditions of the three involved lasers are summarized in Table 1. The driving conditions of the two slave lasers are not identical because each laser is modulated by a different PPG. The PPG that generates the pulses that modulate SL1 delivers a maximum voltage of 2.5 V, while the PPG that modulates SL2 provides a maximum voltage of 1 V. This signal is subsequently amplified such that it shows

TABLE 1. Driving conditions of the lasers and devices.

Description	Symbol	Value
Master laser wavelength	λ_{ML}	1,549.57 nm
Master laser optical power after attenuator	P_{ML}	-11.5 dBm
SL1 DC bias current	I_{SL1}^{DC}	5.1 mA
SL1 AC peak-to-peak voltage	V_{SL1}^{AC}	2.5 V
SL1 AC pulse repetition rate	f_{R1}	100 MHz
SL2 DC bias current	I_{SL2}^{DC}	1.4 mA
SL2 AC peak-to-peak voltage	V_{SL2}^{AC}	3.1 V
SL2 AC pulse repetition rate	f_{R2}	100.01 MHz
AC signal pulse width	t_{pulse}	200 ps
EDFA current	I_{EDFA}	38 mA
Acousto-optic modulator driver frequency	f_{shift}	80 MHz

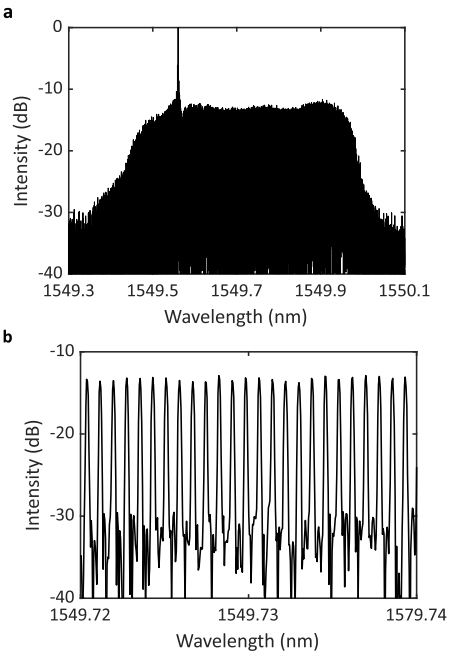

FIGURE 4. One of the two OFCs generated to perform DCS measured with a 10-MHz resolution optical spectrum analyzer. It is obtained by GS the optically-injected DFB laser using a train of pulses with a repetition frequency of 100 MHz. The higher peak, located at 1,549.57 nm, corresponds to the optical injection from the master laser. A 0.02 nm zoom of the absorption region is shown in b.

a peak-to-peak voltage of ∼3.1 V at the input of SL2. The bias currents of the two lasers are optimized in relation to their threshold current and the peak-to-peak voltage of the pulsed signal. In both slave lasers the excitation pulses have a nominal duration of 200 ps, corresponding to a duty cycle of 2%.

The central frequency of both slave lasers is finely tuned using temperature controllers to ensure locking to the master laser and to select a flat comb region at the gas absorption frequencies. Fig. 4 shows, as an example, the OFC generated by SL2 measured with a high-resolution (10 MHz) Brillouin optical spectrum analyzer (Aragon Photonics BOSA 400 C + L). The master laser injection is set at 1,549.57 nm, around 20 GHz away from the gas

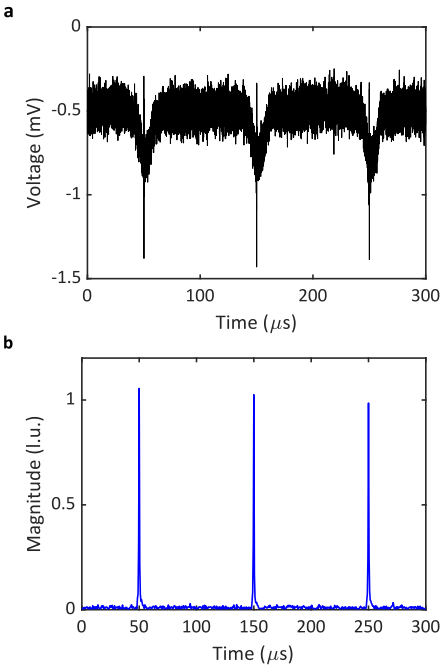

FIGURE 5. a Time-domain interferograms recorded with the oscilloscope. b Interferograms obtained with the SDR platform. The bursts reproduce with a periodicity given by the inverse of the repetition frequency difference of the two combs, 100 μs.

absorption line, to avoid some instabilities observed close to the injection frequency. The OFC shown in Fig. 4 **a** features a large bandwidth of ∼75 GHz within 10 dB (∼750 lines) and a high carrier-to-noise ratio, as defined in [12], of ∼32 dB. A closer look at Fig. 4 **a** shows clearly defined peaks with a flatness better than 2 dB along the gas absorption region (Fig. 4 **b**). Since the repetition frequency, f_R, is 100 MHz, a high number of comb lines lie within the gas absorption line, whose full-width at half maximum (FWHM) is ∼2 GHz. The repetition rate difference is $\Delta f_R = 10$ kHz, i.e. the compression factor ($f_R/\Delta f_R$) is 10,000. Therefore, the RF bandwidth of the SDR platform (3.2 MHz) fits an optical bandwidth of 32 GHz. This bandwidth is large enough to capture the absorption line and to correct the effects of the baseline.

In the time domain, when the two combs beat in the photodetector, interference waveforms (i.e., interferograms) are obtained. Fig. 5 **a** shows the interferograms recorded by the oscilloscope while panel **b** shows the interferograms provided by the SDR platform in terms of the magnitude of the IQ data. The periodicity of the interferograms center-bursts is 100 μs (the inverse of $\Delta f_R = 10$ kHz), as evidenced in both plots. The sampling rate of the oscilloscope is set to 200 Msamples/s and its analog bandwidth is limited to 100 MHz in order to select the first Nyquist zone. Five hundred single shots of 2 ms length are recorded sequentially with the oscilloscope, each of them containing 20 interferograms. The sampling rate of the SDR platform is 2 Msamples/s. With this configuration, temporal traces of 10 ms are recorded. The interferograms recorded with the SDR platform are cleaner due its smaller bandwidth, which reduces the noise.

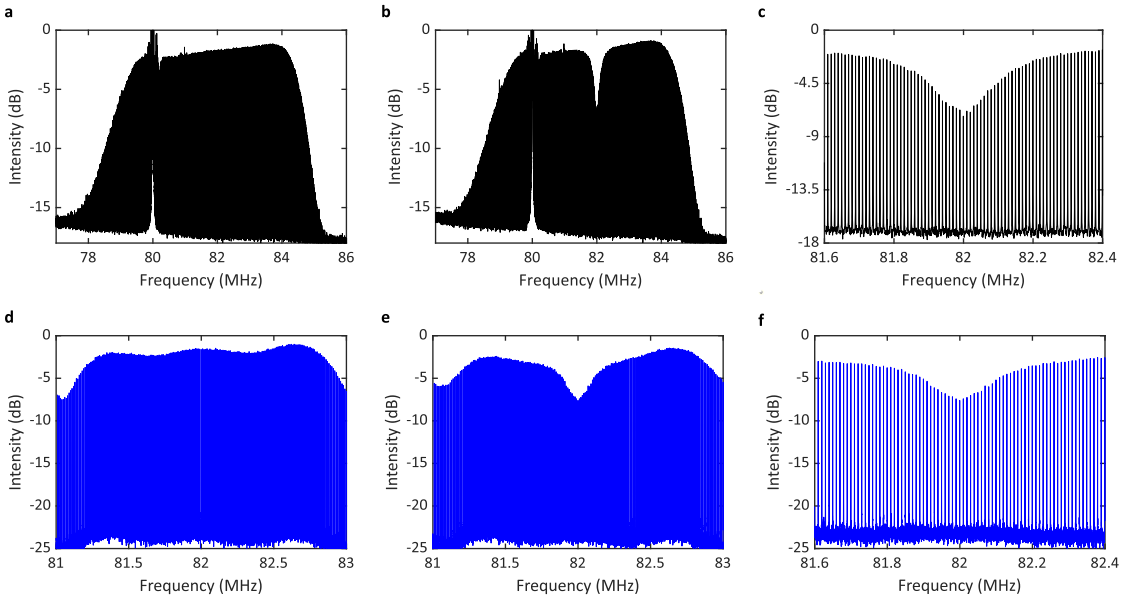

FIGURE 6. Down-converted RF comb spectra obtained from the temporal traces recorded with the oscilloscope (top row, black line graphs) and with the SDR platform (bottom row, blue line plots). The total integration time in both cases is 1 s, achieved averaging 500 spectra in the case of the oscilloscope measurements and 100 spectra in the case of the SDR. A zoom of the absorption line footprint is shown in c and f.

Fig. 6 shows the down-converted RF spectra obtained after performing the Fourier transform of the time-domain interferograms digitized with the oscilloscope (Fig. 5 **a**) and with the SDR platform (Fig. 5 **b**). In the case of the SDR platform, the complex IQ data are used for the Fourier transform. The spectra shown on the left panels (Fig. 6 **a**, **d**) are the reference ones. Next to them, the spectra obtained when the optical signal passes through the gas cell are depicted in panels **b** and **e**. For all these measurements, the total integration time is 1 s, corresponding to five hundred 2-ms-long single shots of the oscilloscope and to one hundred 10-ms-long traces in the SDR platform. In both cases the averaging is performed in the spectral domain. The RF spectra measured with the oscilloscope show the complete down-converted comb with around 640 lines in 10 dB and a good flatness for absorption measurements. The peak at 80 MHz corresponds to the master laser injection, as the acousto-optic modulator shifts by 80 MHz what was the common reference of both slave lasers. The feature of the absorption line at 82 MHz is clearly visible in Fig. 6 **c**, **f**. The previously commented instabilities at the injection wavelength give rise to the additional harmonics close to 80 MHz shown in Fig. 6 **a**, **b**. The origin of these harmonics has not been investigated.

The working principle of SDR platforms is very appropriate for this kind of measurements, as they shift the center frequency of the signal with a tunable analog local oscillator before digitizing [28], thus allowing the use of lower sampling rates than the required for directly sampling the signal. The local oscillator frequency is configured by the RF center frequency parameter, defined in the software interface. In this case, the RF center frequency is set to 82 MHz, and a 2 MHz bandwidth is more than enough to properly measure the absorption line (see Fig. 6 **e**). In these acquisition conditions, the resolution of the measurement is as high as 10 Hz and therefore, a proper characterization of the comb tones of 100 MHz is fully guaranteed. Fig. 6 **f** shows a zoom of panel **e**, where the individual lines are very well resolved and a carrier-to-noise ratio of around 20 dB can be observed, which is a very good value for this comb, indicating a very high degree of mutual coherence between the two optical combs. The transmission profile of the absorption line is obtained by normalizing the RF spectrum that contains the gas information with a reference measurement. A linear baseline correction is applied to the obtained transmission curve. In addition, a Voigt function is fitted to the line profile. The experimental profiles of the $H^{13}C^{14}N$ P(10) line recorded with the oscilloscope and the SDR for three integration times are presented in Fig. 7. Panels **a**, **b** and **c** show the results obtained with the oscilloscope for integration times of 100 ms, 500 ms, and 1 s, respectively. The residuals from the Voigt fitting process can be observed in the bottom part of each figure. For the longest integration time, the absorption depth and the linewidth provided by the fit are $T = 0.54$ and FWHM $= 2.3$ GHz, respectively. These values are in good agreement with the transmission data provided by the NIST [29] and the linewidth information provided by the gas cell manufacturer. The standard deviation of the residuals (σ_{res}) calculated in a 15.6 GHz span is 0.84%. The transmission results obtained with the SDR platform, together with the corresponding residuals, are shown in Fig. 7 **d**, **e** and **f** for the same integration times as those of the oscilloscope measurements. For an integration time of 1 s, the minimum transmission measured from the fitting curve and the linewidth are 0.54 and 2.4 GHz, respectively, also very close to the expected values. In this case, the residuals are slightly higher, $\sigma_{res} = 0.97\%$.

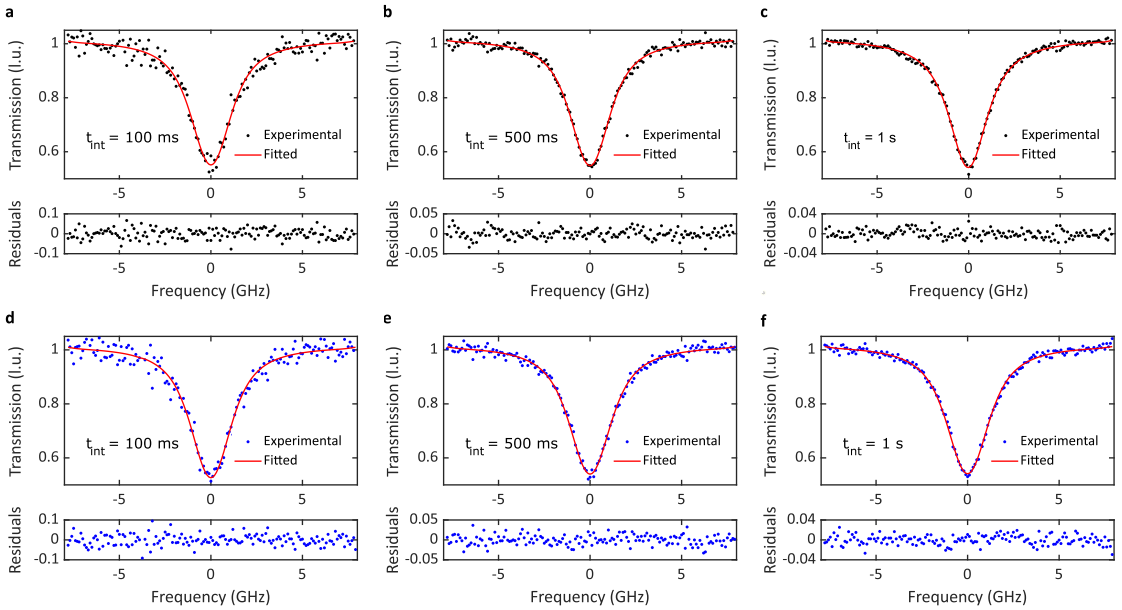

FIGURE 7. Transmission profiles of the $H^{13}C^{14}N$ P(10) line. The black dots plot the profile obtained experimentally and the solid red line corresponds to the Voigt profile fitted to these data. The residuals from the fitting are shown in the bottom part of each figure. The results acquired using the oscilloscope to digitize the data are shown in the top row for integration times (t_{int}) of: a, 100 ms; b, 500 ms and c, 1 s. The transmittances obtained for these same integration times when the acquisition is performed with the SDR platform are shown in the bottom row: d, e and f.

Our results demonstrate the advantages of using SDR platforms, instead of the usual digitizers, for recording and analyzing the RF spectra in DCS. It is worth noting that the usefulness of these receivers should not be restricted to the dual combs generated by these relatively narrow OFCs. For instance, using the same SDR and assuming the same mutual coherence leading to 10-Hz-narrow RF tones, a spectrum as wide as 32 THz could fit into the 3.2 MHz bandwidth of the SDR by using a compression factor 10^7 ($f_R = 100$ MHz, $\Delta f_R = 10$ Hz). Additionally, for acquiring a RF spectrum broader than 3.2 MHz using this SDR platform, the center frequency can be sequentially tuned in order to capture the different regions of the spectrum. Of course, this would be detrimental to the acquisition speed. Alternatively, other affordable SDR platforms offering higher bandwidths than the one discussed here could be used.

IV. CONCLUSION

We have demonstrated the performance as a receiver of a SDR platform in comparison with a high-end real-time oscilloscope in a DCS system based on GS semiconductor lasers. This demonstration points in the direction of the possibility of using low-cost SDR platforms in the receiver end of dual-comb spectrometers. This approach is a step forward in the quest for low-cost, field deployable dual-comb spectrometers. The cost-efficiency of our solution would be improved by replacing the EDFA and the high-bandwidth photodetector by a commercial photodetector with a transimpedance amplifier and a bandwidth adequate to this application (100 MHz). In combination with low-cost excitation sources such as step-recovery diodes and integrated optical sources, our approach could contribute to pave the way towards a good number of gas sensing and other applications of dual-comb architectures requiring an affordable technology.

ACKNOWLEDGMENT

Antonio Pérez-Serrano would like to thank J. M. García-Loygorri (ETSIST-UPM) for useful discussions about SDR platforms.

REFERENCES

[1] S. A. Diddams, K. Vahala, and T. Udem, "Optical frequency combs: Coherently uniting the electromagnetic spectrum," *Science*, vol. 369, no. 6501, Jul. 2020, Art. no. eaay3676. [Online]. Available: https://science.sciencemag.org/content/369/6501/eaay3676

[2] I. Coddington, W. Swann, and N. Newbury, "Coherent multiheterodyne spectroscopy using stabilized optical frequency combs," *Phys. Rev. Lett.*, vol. 100, no. 1, Jan. 2008, Art. no. 013902. [Online]. Available: https://link.aps.org/doi/10.1103/PhysRevLett.100.013902

[3] M. Imran, P. M. Anandarajah, A. Kaszubowska-Anandarajah, N. Sambo, and L. Potí, "A survey of optical carrier generation techniques for terabit capacity elastic optical networks," *IEEE Commun. Surveys Tuts.*, vol. 20, no. 1, pp. 211–263, 1st Quart., 2018.

[4] M. Piccardo, M. Tamagnone, B. Schwarz, P. Chevalier, N. A. Rubin, Y. Wang, C. A. Wang, M. K. Connors, D. McNulty, A. Belyanin, and F. Capasso, "Radio frequency transmitter based on a laser frequency comb," *Proc. Nat. Acad. Sci. USA*, vol. 116, no. 19, pp. 9181–9185, May 2019. [Online]. Available: https://www.pnas.org/content/116/19/9181

[5] Z. Zhu and G. Wu, "Dual-comb ranging," *Engineering*, vol. 4, no. 6, pp. 772–778, Dec. 2018. [Online]. Available: http://www.sciencedirect.com/science/article/pii/S2095809918303783

[6] X. Xu, Z. Zhang, H. Zhang, H. Zhao, W. Xia, M. He, J. Li, J. Zhai, and H. Wu, "Long distance measurement by dynamic optical frequency comb," *Opt. Exp.*, vol. 28, no. 4, pp. 4398–4411, Feb. 2020. [Online]. Available: http://www.opticsexpress.org/abstract.cfm?URI=oe-28-4-4398

[7] P. Trocha, M. Karpov, D. Ganin, M. H. P. Pfeiffer, A. Kordts, S. Wolf, J. Krockenberger, P. Marin-Palomo, C. Weimann, S. Randel, W. Freude, T. J. Kippenberg, and C. Koos, "Ultrafast optical ranging using microresonator soliton frequency combs," *Science*, vol. 359, no. 6378, pp. 887–891, Feb. 2018. [Online]. Available: https://science.sciencemag.org/content/359/6378/887

[8] N. Picqué and T. W. Hänsch, "Frequency comb spectroscopy," *Nature Photon.*, vol. 13, no. 3, pp. 146–157, 2019.

[9] I. Coddington, N. Newbury, and W. Swann, "Dual-comb spectroscopy," *Optica*, vol. 3, no. 4, pp. 414–426, Apr. 2016. [Online]. Available: http://www.osapublishing.org/optica/abstract.cfm?URI=optica-3-4-414

[10] R. Zhou, S. Latkowski, J. O'Carroll, R. Phelan, L. P. Barry, and P. Anandarajah, "40 nm wavelength tunable gain-switched optical comb source," *Opt. Exp.*, vol. 19, no. 26, pp. B415–B420, Dec. 2011. [Online]. Available: http://www.opticsexpress.org/abstract.cfm?URI=oe-19-26-B415

[11] P. M. Anandarajah, S. P. Ó. Dúill, R. Zhou, and L. P. Barry, "Enhanced optical comb generation by gain-switching a single-mode semiconductor laser close to its relaxation oscillation frequency," *IEEE J. Sel. Topics Quantum Electron.*, vol. 21, no. 6, pp. 592–600, Nov. 2015.

[12] A. Rosado, A. Pérez-Serrano, J. M. G. Tijero, Á. Valle, L. Pesquera, and I. Esquivias, "Experimental study of optical frequency comb generation in gain-switched semiconductor lasers," *Opt. Laser Technol.*, vol. 108, pp. 542–550, Dec. 2018. [Online]. Available: http://www.sciencedirect.com/science/article/pii/S003039921830820X

[13] R. Zhou, T. N. Huynh, V. Vujicic, P. M. Anandarajah, and L. P. Barry, "Phase noise analysis of injected gain switched comb source for coherent communications," *Opt. Exp.*, vol. 22, no. 7, pp. 8120–8125, Apr. 2014. [Online]. Available: http://www.opticsexpress.org/abstract.cfm?URI=oe-22-7-8120

[14] A. Rosado, A. Pérez-Serrano, J. M. G. Tijero, A. V. Gutierrez, L. Pesquera, and I. Esquivias, "Numerical and experimental analysis of optical frequency comb generation in gain-switched semiconductor lasers," *IEEE J. Quantum Electron.*, vol. 55, no. 6, pp. 1–12, Dec. 2019.

[15] A. Rosado, A. Pérez-Serrano, J. M. G. Tijero, Á. Valle, L. Pesquera, and I. Esquivias, "Enhanced optical frequency comb generation by pulsed gain-switching of optically injected semiconductor lasers," *Opt. Exp.*, vol. 27, no. 6, pp. 9155–9163, Mar. 2019. [Online]. Available: http://www.opticsexpress.org/abstract.cfm?URI=oe-27-6-9155

[16] C. Quevedo-Galán, V. Durán, A. Rosado, A. Pérez-Serrano, J. M. G. Tijero, and I. Esquivias, "Gain-switched semiconductor lasers with pulsed excitation and optical injection for dual-comb spectroscopy," *Opt. Exp.*, vol. 28, no. 22, p. 33307, 2020.

[17] J. K. Alexander, L. Caro, M. Dernaika, S. P. Duggan, H. Yang, S. Chandran, E. P. Martin, A. A. Ruth, P. M. Anandarajah, and F. H. Peters, "Integrated dual optical frequency comb source," *Opt. Exp.*, vol. 28, no. 11, pp. 16900–16906, May 2020. [Online]. Available: http://www.opticsexpress.org/abstract.cfm?URI=oe-28-11-16900

[18] A. Rosado, E. P. Martin, A. Pérez-Serrano, J. M. G. Tijero, I. Esquivias, and P. M. Anandarajah, "Optical frequency comb generation via pulsed gain-switching in externally-injected semiconductor lasers using step-recovery diodes," *Opt. Laser Technol.*, vol. 131, Nov. 2020, Art. no. 106392. [Online]. Available: https://www.sciencedirect.com/science/article/pii/S0030399220310252

[19] C. A. Michal, "A low-cost multi-channel software-defined radio-based NMR spectrometer and ultra-affordable digital pulse programmer," *Concepts Magn. Reson. B, Magn. Reson. Eng.*, vol. 48B, no. 3, Jul. 2018, Art. no. e21401. [Online]. Available: https://onlinelibrary.wiley.com/doi/abs/10.1002/cmr.b.21401

[20] A. Doll, "Pulsed and continuous-wave magnetic resonance spectroscopy using a low-cost software-defined radio," *AIP Adv.*, vol. 9, no. 11, Nov. 2019, Art. no. 115110, doi: 10.1063/1.5127746.

[21] P. Mahnke, "Characterization of a commercial software defined radio as high frequency lock-in amplifier for FM spectroscopy," *Rev. Sci. Instrum.*, vol. 89, no. 1, Jan. 2018, Art. no. 013113, doi: 10.1063/1.4999552.

[22] L. M. Riobó, F. E. Veiras, M. T. Garea, and P. A. Sorichetti, "Software-defined optoelectronics: Space and frequency diversity in heterodyne interferometry," *IEEE Sensors J.*, vol. 18, no. 14, pp. 5753–5760, Jul. 2018.

[23] M. Čížek, V. Hucl, J. Hrabina, R. Šmíd, B. Mikel, J. Lazar, and O. Číp, "Two-stage system based on a software-defined radio for stabilizing of optical frequency combs in long-term experiments," *Sensors*, vol. 14, no. 1, pp. 1757–1770, Jan. 2014.

[24] D. A. Long, A. J. Fleisher, K. O. Douglass, S. E. Maxwell, K. Bielska, J. T. Hodges, and D. F. Plusquellic, "Multiheterodyne spectroscopy with optical frequency combs generated from a continuous-wave laser," *Opt. Lett.*, vol. 39, no. 9, pp. 2688–2690, May 2014. [Online]. Available: http://ol.osa.org/abstract.cfm?URI=ol-39-9-2688

[25] *RTL-SDR.COM Blog*. Accessed: Apr. 22, 2021. [Online]. Available: http://www.rtl-sdr.com

[26] W. Kadman. (Mar. 2013). *R820T Rafael Micro—High Performance Low Power Advanced Digital TV Silicon Tuner*. Accessed: Apr. 22, 2021. [Online]. Available: http://radioaficion.com/cms/r820t-rafael-micro/

[27] RealTek. *RTL2832U DVB-T COFDM Demodulator + USB 2.0*. Accessed: Apr. 22, 2021. [Online]. Available: https://www.realtek.com/en/products/communications-network-ics/item/rtl2832u

[28] R. Stewart, K. Barlee, and D. Atkinson, *Software Defined Radio Using MATLAB & Simulink and the RTL-SDR*. Glasgow, Scotland: Strathclyde Academic Media, 2015. [Online]. Available: https://books.google.es/books?id=swp0awEACAAJ

[29] S. Gilbert, W. Swann, and C. Wang, *Hydrogen Cyanide $H^{13}C^{14}N$ Absorption Reference for 1530 nm to 1565 nm Wavelength Calibration*, Standard SRM 2519a, Aug. 2005.

CLARA QUEVEDO-GALÁN was born in Tomelloso, Spain, in 1994. She received the B.S. degree in telecommunication engineering and the M.Sc. degree in photonics engineering from the Universidad Politécnica de Madrid, Spain, in 2018 and 2019, respectively, where she is currently pursuing the Ph.D. degree. Since 2019, she has been a Research Fellow with the CEMDATIC-E.T.S.I. Telecomunicación, Universidad Politécnica de Madrid. Her research interest includes optical frequency combs generated with semiconductor lasers and their applications, with special emphasis in dual-comb spectroscopy.

ANTONIO PÉREZ-SERRANO was born in Badalona, Spain, in 1978. He received the Ph.D. degree in physics from the Universitat de les Illes Balears, Palma de Mallorca, Spain. He is currently an Assistant Professor with the Universidad Politécnica de Madrid, Spain. His research interests include photonic integrated circuits and semiconductor lasers, with particular emphasis in multi-mode dynamics, and ring lasers and multi-section lasers.

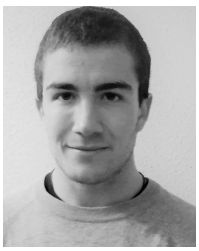

IGNACIO E. LÓPEZ-DELGADO was born in Madrid, Spain, in 1998. He received the degree in telecommunication engineering from the Universidad Politécnica de Madrid, Spain, in 2020, where he is currently pursuing the degree. He is currently a Research Intern with the Universidad Politécnica de Madrid. His research interests include dual-comb spectroscopy and LiDAR systems.

JOSE MANUEL G. TIJERO was born in Burgos, Spain, in 1960. He received the M.Sc. degree in physics from the Universidad de Zaragoza, in 1984, and the Ph.D. degree in physics from the Universidad Autónoma de Madrid, in 1989. Since 1994, he has been an Associate Professor with the Universidad Politécnica de Madrid.

IGNACIO ESQUIVIAS was born in Madrid, Spain, in 1955. He received the M.Sc. and Ph.D. degrees in electronic engineering from the Universidad Politécnica de Madrid, in 1977 and 1983, respectively. He became a Full Professor with the Universidad Politécnica de Madrid, in 2001. He leads the Laser Diode Group, CEMDATIC-E.T.S.I. Telecomunicación, with activity in laser diode modeling and characterization, since 1992.